Eur. Phys. J. E (2015) **38**: 78
DOI 10.1140/epje/i2015-15078-3

THE EUROPEAN PHYSICAL JOURNAL E

Regular Article

Stabilising lamellar stacks of lipid bilayers with soft confinement and steric effects

K. Bougis[1], R. Leite Rubim[2], N. Ziane[1], J. Peyencet[1], A. Bentaleb[1], A. Février[1], C.L.P. Oliveira[2], E. Andreoli de Oliveira[2], L. Navailles[1], and F. Nallet[1,a]

[1] Université de Bordeaux, Centre de recherche Paul-Pascal–CNRS, 115 avenue du Docteur-Schweitzer, F-33600 Pessac, France
[2] Universidade de São Paulo, Instituto de Física-GFCx, P.O.B. 66318, São Paulo, SP 05314-970, Brazil

Received 16 December 2014 and Received in final form 17 April 2015
Published online: 16 July 2015 – © EDP Sciences / Società Italiana di Fisica / Springer-Verlag 2015

Abstract. Structure and interactions stabilising the lamellar stack of mixed lipid bilayers in their fluid state are investigated by means of small-angle X-ray scattering. The (electrically neutral) bilayers are composed of a mixtures of lecithin, a zwitterionic phospholipid, and Simulsol, a non-ionic cosurfactant with an ethoxylated polar head. The soft confinement of the bilayer hydrophilic components is varied by changing hydration and bilayer composition, as well as the length of the cosurfactant polar head. Structural transitions are observed at low hydration, in the stacking order for the longer cosurfactant, and in the mixed bilayers for the shorter one. At higher hydration, the swelling of the lamellar stacks occurs with a significant, but continuous evolution in the mixed bilayer structure. The bilayer structural changes are discussed in analogy with the so-called "brush-to-mushroom" transition induced by lateral confinement, relevant for long linear polymers grafted onto rigid surfaces, taking also into account the role of vertical confinement.

1 Introduction

From mixture of lipids and water, multilamellar systems may naturally emerge. In such self-assembled systems, a periodic structure is formed by stacking lipid bilayers and layers of water. In the case where there is no in-plane order in the bilayers—in their so-called "fluid state"—the system exhibits the symmetry of a smectic A phase, commonly referred to as a lamellar L_α phase in the context of lipid materials.

Local (bilayer), as well as global phase properties may be altered by mixing lipids with other amphiphilic molecules, surfactants or amphiphilic polymers for instance, one motivation being the design of, *e.g.*, biosensors [1–4] or delivery systems in the form of liposomes [3, 5, 6].

In view of tailoring the targeted applications of the resulting multilamellar lipid stacks, it is often convenient to describe the effects of altering the bilayer composition in terms of *physical* properties such as bilayer curvature elasticity and inter-bilayer interactions. Since the seminal paper by W. Helfrich theoretically introducing steric (also known as *undulation*) interactions in multilayer systems [7], and the first experimental evidence for the undulation mechanism [8, 9], such an approach has been quite fruitful. For instance, in line with the theoretical prediction given in ref. [10], adding a co-surfactant (1-pentanol) to a dimyristoyl phosphatidylcholine-based lamellar system was shown to strikingly decrease the bilayer bending modulus κ from a value of, typically, $25k_BT$ [11] to $\approx k_BT$ [12] with, as a consequence of the resulting enhanced steric repulsion between bilayers, a spectacular increase of the dilution limit of the lamellar stack. Manipulating electrostatic interactions, or various kinds of polymer-induced steric inter-bilayer interactions have accordingly been the subject of numerous studies, both from the theoretical [13–18] and experimental [19–22] points of view.

Here, we study with the above-described perspective a lecithin-based lamellar system in the presence of a non-ionic co-surfactant, a system which has shown its ability to efficiently encapsulate DNA fragments in spite of the absence of any obvious direct electrostatic mechanism at play [23–25]. The co-surfactant we use is an ethoxylated fatty acid, *i.e.* a (short) non-ionic block copolymer with amphiphilic properties. The present work expands ref. [26], with a better control of the steric effects on both curvature elasticity and interactions as we now use *size-sorted* co-surfactant molecules.

The lamellar structure of the stacked bilayers is characterised by means of small-angle X-ray scattering, polarised light microscopy being also used as a complementary technique. Diffractograms are analysed in terms of the model described in ref. [27], with improvements of the fitting procedure as in ref. [28]. Bending elasticity of individual

[a] e-mail: nallet@crpp-bordeaux.cnrs.fr

bilayers, as well as inter-bilayer interactions are characterised by the value of the Caillé parameter η extracted from data analysis, the latter also yielding both in-plane and normal information about the bilayer structure at the molecular scale.

The Caillé parameter, defined in terms of the two elastic constants of a smectic A liquid crystal, namely the splay constant K and the smectic layer compression modulus B by [29]

$$\eta = \frac{q_0^2 k_B T}{8\pi\sqrt{KB}} \tag{1}$$

is indeed useful in assessing bilayer physical properties as, in simple limiting cases, the smectic splay constant K and the bilayer bending modulus κ are related by [7]

$$K = \frac{\kappa}{\ell}\,, \tag{2}$$

with $\ell \equiv 2\pi/q_0$ the smectic period, while the following equation relates the smectic compression modulus B to the inter-bilayer interaction potential $V(\ell)$ (potential energy per unit bilayer area, loosely speaking, but to be more correctly designated as the *free energy* per unit bilayer area of the bilayer stack) [7, 9, 30, 31]

$$B = \ell \frac{\partial^2 V}{\partial \ell^2}\,. \tag{3}$$

We are interested in the effects of *confinement* on bilayer physical properties (as encapsulated in η values and bilayer structure), where confinement, ultimately originating from local steric repulsive interactions, is to be understood along both stacking (vertical, z) and in-plane (lateral, $\perp$) directions: Vertical confinement is varied by controlling the hydration of the lamellar stack (as in refs. [24, 25]), but also by changing the molecular length of the co-surfactant ethoxylated part—see below sect. 2.1. Lateral confinement is primarily controlled by the co-surfactant amount in the lipid bilayer—loosely speaking, co-surfactant "grafting density" in analogy with systems of polymer brushes [32]. It also indirectly depends on z-confinement, as already suggested in ref. [26].

2 Materials and methods

2.1 Sample preparation

Soya lecithin (from Sigma-Aldrich) is a phosphatidylcholine (PC) lipid with a fatty acid component mostly composed of linoleic acid (64%). As choline and phosphate groups bear opposite electric charges, this lipid is zwitterionic. Its average molar mass is around $776\,\mathrm{g\,mol^{-1}}$. The hydrophobic part of the Simulsol (from Seppic) co-surfactants considered here is oleic acid, and is therefore commensurate with the hydrophobic tails of the lipid. We use here two Simulsols differing by their *hydrophilic* parts, with either 16 or 6 ethoxylated monomers -$CH_2 - CH_2$-O- and corresponding molar masses $987\,\mathrm{g\,mol^{-1}}$ or $547\,\mathrm{g\,mol^{-1}}$. These compounds will be referred to as, respectively, Simulsol $n = 16$ and Simulsol $n = 6$. Though tailored by the supplier for having the specified lengthes, these Simulsols have (unknown) dispersities that are *a priori* comparable to the dispersity of Simulsol 2599 PHA used for sample preparation in previous studies [24–26]. Simulsol 2599 PHA will be later referred to as Simulsol $\langle n\rangle = 10$, as it contains 10 ethoxylated monomers on average, in a range extending from ca. $n = 5$ to $n = 20$ according to the supplier.

We prepare mixtures of lecithin and Simulsol at the desired composition by cosolubilizing lipids and surfactants in cyclohexane, lyophilisation for about a day being then used to remove the organic solvent. Pure water in appropriate amounts for reaching the desired hydration is further added to the lyophilate. Samples are centrifuged, typically twice a day for 10 minutes and at 2500 rpm, during at least one week and conserved at 4 °C between centrifuge cycles in order to reach homogeneity, checked visually. In this way, we formulate different bilayer compositions by varying the lecithin/Simulsol molar content, as well as the Simulsol length. With Simulsol $n = 16$, only one composition was prepared, namely L80/S20 in terms of the lecithin/Simulsol molar ratio, a value close to the one already chosen in previous studies [24–26]. The bilayer compositions chosen with Simulsol $n = 6$ are the following: L89/S11, L62/S38, L56/S44, L37/S63, L27/73 and L0/S100. We later use the total lecithin plus Simulsol volume fraction ϕ_{lip} (water volume fraction $1 - \phi_{\mathrm{lip}}$) in addition to the L/S molar ratio for describing sample compositions.

2.2 Microscope observation

For all the samples studied, we have recorded images in polarised light microscopy with moderate magnification (data not shown) as lamellar phases should be optically anisotropic. We used a Olympus BX 51 microscope with crossed polarizers for observing samples sandwiched between a glass slide and a coverslip, without special precautions for ensuring a constant optical path but preventing water evaporation by means of a UV-curing glue. A weakening birefringence as hydration increases is always observed, without obvious indications of any kind of phase coexistence for the samples later retained for structural characterisations.

2.3 X-ray scattering

Equilibrated samples are introduced into cylindrical quartz capillaries with a nominal diameter 1.5 mm that are further flame-sealed. Diffractograms are recorded on a Bruker Nanostar machine equipped with a Hi-Star detector, also from Bruker. A crossed-coupled pair of Göbel mirrors (Bruker) selects the $\lambda = 1.5418$ Å radiation of a Copper source (Siemens) operated at 40 kV and 35 mA. A 3-pinhole system is used for collimating the incident beam, with a size (FWHM) at sample position ca. 0.43 mm

in both vertical and horizontal directions. The sample-to-detector distance, found close to 0.25 m, is calibrated using Silver behenate as standard. From the Gaussian width of the first order Bragg peak of Silver behenate, we estimate a resolution width (FWHM) $\Delta q \approx 2.0 \times 10^{-2}\,\text{Å}^{-1}$. The scattering wave vectors that are practically accessible after subtracting the signal of a reference (water) capillary range from $0.04\,\text{Å}^{-1}$ to $0.8\,\text{Å}^{-1}$.

For accessing to higher scattering wave vector values (typically 0.12–$2.2\,\text{Å}^{-1}$), we use a custom-made instrument with a Copper rotating-anode–based setup and crossed-coupled pair of Göbel mirrors, both from Rigaku, 3-pinhole collimation and a mar345 image plate detector (marXperts GmbH). At contrast with the Bruker system, only the collimation flight path is evacuated.

Acquisition times on both instruments are typically 2 to 4 hours, depending on the hydration level of samples. Temperature, fixed at 20 °C, is controlled to within ±0.2 °C by a water circulation system. The 2D detector images are most often characteristic of unoriented samples, and data is therefore azimuthally averaged to yield (normalised) intensities I *vs.* scattering wave vector q curves.

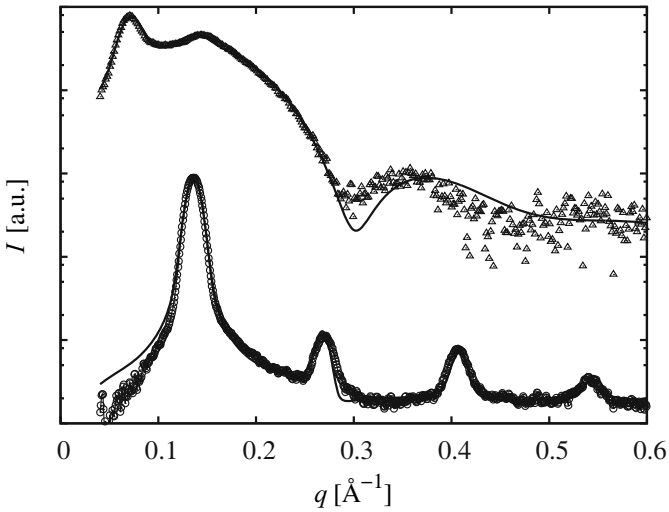

Fig. 1. Characteristic diffractograms in the concentrated (○, $\phi_{\text{lip}} = 0.86$) and diluted (△, $\phi_{\text{lip}} = 0.37$) regimes for Simulsol $n = 6$ and bilayer composition L37/S63. The data point dispersion around the "mean" features of both diffractograms is representative of the measurement errors for the (background-corrected) scattered intensities. Errors are consistently larger for low-scattering regions and the less concentrated sample. Fitted values found for the $\phi_{\text{lip}} = 0.86$ (respectively, $\phi_{\text{lip}} = 0.37$) sample: $\ell = 4.61\,\text{nm}$, $\eta = 9 \times 10^{-3}$, $\delta_H = 1.34\,\text{nm}$, $\delta_T = 0.99\,\text{nm}$ and $r_\rho = -1.25$ (respectively, $\ell = 8.8\,\text{nm}$, $\eta = 0.35$, $\delta_H = 1.23\,\text{nm}$, $\delta_T = 0.99\,\text{nm}$ and $r_\rho = -1.50$).

3 Experimental results and discussion

3.1 General features

For all the studied samples, the mixed lipid-surfactant bilayer is in its fluid (L_α) state, as evidenced by the presence of a broad peak in scattered intensity centred at $1.4\,\text{Å}^{-1}$, characteristic of the disordered packing of aliphatic chains at the molecular scale (data not shown). This kind of packing is expected at room temperature for C18 aliphatic chains bearing unsaturated bonds. At high hydration levels, a hump gradually appearing at about $1.8\,\text{Å}^{-1}$ as ϕ_{lip} decreases becomes a separate broad peak. It corresponds to the liquid phase of water.

At larger scales, the periodic stacking of the fluid bilayers in a lamellar phase is evidenced by the presence of 2 to 4 Bragg peaks associated to wave vectors in the sequence (1:2:3:4), except for a range of rather dehydrated samples with Simulsol $n = 16$ where two distinct sets of separately regularly spaced Bragg peaks indicate a phase *coexistence* between "swollen" and "collapsed" lamellar structures. Note that phase separation is *not* observed at the macroscopic scale in the corresponding sample vials, nor with polarised optical microscopy, a feature not uncommon at low hydration in lamellar stacks of surfactant bilayers [21].

Qualitatively speaking, it is possible to split the diffractograms for one-phase samples in two categories, one associated to lipid volume fraction ϕ_{lip} larger than ~ 0.65, where, as will be detailed below, bilayers are "confined", the second category being associated to more hydrated systems, and "swollen" bilayers. As displayed for illustration in fig. 1, a larger number of better defined Bragg peaks, together with less diffuse intensity are characteristic for the lamellar stacking of "confined" bilayers, while the reverse is true for "swollen" bilayers. There is no obvious effect of the Simulsol length, nor of the Simulsol fraction on the existence of the two categories and the boundary between categories does not vary strongly either. In the particular case of the *phase coexistence* which is observed for $0.75 \geq \phi_{\text{lip}} \geq 0.60$ with Simulsol $n = 16$ and bilayer composition L80/S20, the small-angle scattering data may be considered as resulting from a weighted combination of "confined" and "swollen" diffractograms, with a decreasing weight for the "confined" component as hydration increases. Note that a comparable phase coexistence was observed in a similar, though narrower, hydration range with Simulsol $\langle n \rangle = 10$ [26]. Long hydrophilic co-surfactant heads might therefore be responsible for the phase separation phenomenon, whereas short heads could stabilise the one-phase lamellar domain in the phase diagram.

All the recorded diffractograms are fairly well described by the standard interplay between form factor (diffuse scattering) and structure factor (Bragg scattering) features of our model [27], as shown by the fitted continuous lines in fig. 1 (see[1]). This indicates that, in spite of its known intrinsic limitations at very small angles (where the finite size of the scattering domains becomes an

[1] As a technical remark, it is worth mentioning that, despite an apparent larger departure of the fitted curve from the experimental data for the less concentrated sample in fig. 1, fit "qualities"—as they are defined in ref. [28]—are comparable all along dilution curves for a given bilayer composition.

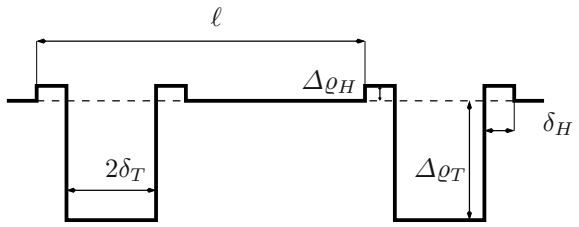

Fig. 2. Schematic representation of the electron density profile along z according to the double square well model.

issue), as well as at large angles (where incompressibility and Porod approximations no longer hold and molecular details should be accounted for), the model description in terms of a *structurally* two-component system, namely bilayer and solvent, remains satisfactory. Apart from the stacking period ℓ which, by the way, is most often also directly read with a good accuracy from the scattering data, the model gives the values for the following fitted parameters: Caillé parameter η, eq. (1), heights δ_H and δ_T along z—as far as the scattering contrast is concerned—of the hydrophilic (head) and hydrophobic (tail) components of half a bilayer and $r_\rho \equiv \Delta\varrho^T/\Delta\varrho^H$, ratio between, respectively, the electronic densities—relative to solvent—of the tail ($\Delta\varrho^T$) and of the head ($\Delta\varrho^H$) components of the bilayer—refer to fig. 2 for a schematic representation of the corresponding electron density profile. The internal consistency of the model obviously requires $2(\delta_T + \delta_H) < \ell$ to be obeyed. Apart from exceptional cases, limited to at worst two of the less hydrated samples in a given series of typically 15 samples[2], this inequality always holds true.

3.2 Dilution laws

The so-called dilution laws, or evolution of the stacking parameter ℓ with hydration for a given bilayer composition, exhibit quite conspicuous features, as shown in fig. 3 (effect of hydrophilic chain length) and fig. 4 (effect of bilayer composition). Except in the case of the L0/S100 system, *i.e. pure* Simulsol $n = 6$ bilayers, the inverse proportionality between ℓ and $\phi_{\rm lip}$ associated to the simple geometric model where constant thickness and identical platelets, parallel to each other, are periodically stacked in space is never observed. The straight line that approximately describes the dilution law at low hydration for Simulsol $n = 6$ in fig. 3 should not be misinterpreted in simple geometric terms, because it does not go through the origin, as it should, if ℓ were actually proportional to $\phi_{\rm lip}^{-1}$ (dotted line in fig. 3). More elaborate geometric models have been proposed to account for deviations from the "ideal" dilution law, for instance by considering the excess area stored in the thermal undulations of the bilayers [33]. Though generically weak, this latter effect has been experimentally reported for very flexible bilayer stacks [34–36], but it is not relevant here for the reason already given in ref. [26]: The deviations we observe are *below*, instead of being above the "ideal" law—as would be the case if excess area were stored in undulations. We therefore propose an alternative geometric interpretation that takes explicitly into account the *lateral* compressibility of the (two-component) bilayers, nevertheless considered for simplicity to remain *flat*. Consider a piece of bilayer with area $\mathcal{A}$ within a lamellar structure of stacking parameter ℓ. It is built by the self-assembly of N_L, respectively N_S, molecules of type L (respectively S) with molecular volume v_L (respectively v_S), a single molecule occupying an area Σ_L (respectively Σ_S) at any of the two bilayer-solvent

[2] The corresponding samples have of course been excluded from all the remaining discussions.

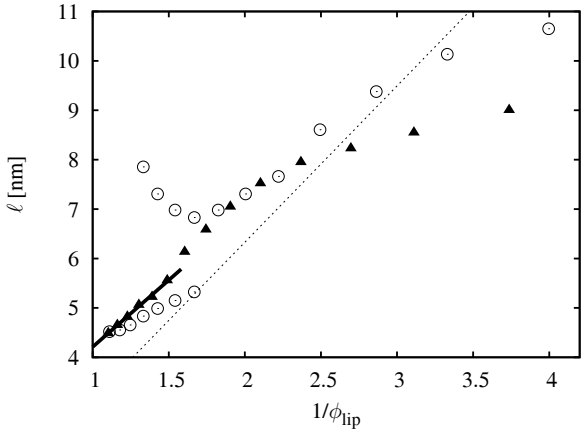

Fig. 3. Dilution law for systems with different Simulsol hydrophilic heads: $n = 16$ (○), $n = 6$ (▲). Bilayer compositions L80/S20 and L56/S44, respectively. With Simulsol $n = 16$, there is a phase coexistence at low overall hydration between "collapsed" and "swollen" lamellar phases. Dotted (respectively, continuous) lines are linear fits constrained to go through the origin (respectively unconstrained) to the whole (respectively low hydration part) $n = 6$ data.

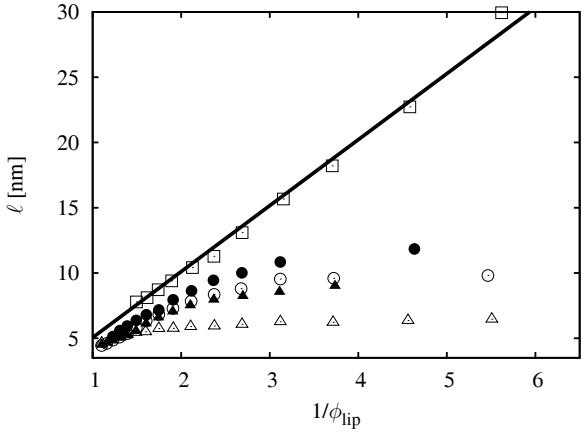

Fig. 4. Dilution law for the system with Simulsol $n = 6$ and various bilayer compositions: L89/S11 (△), L56/S44 (▲), L37/S63 (○), L27/S73 (●) and L0/S100 (□). The continuous line corresponds to the geometric law $\ell = \delta/\phi_{\rm lip}$ with a bilayer thickness $\delta \approx 5.1$ nm.

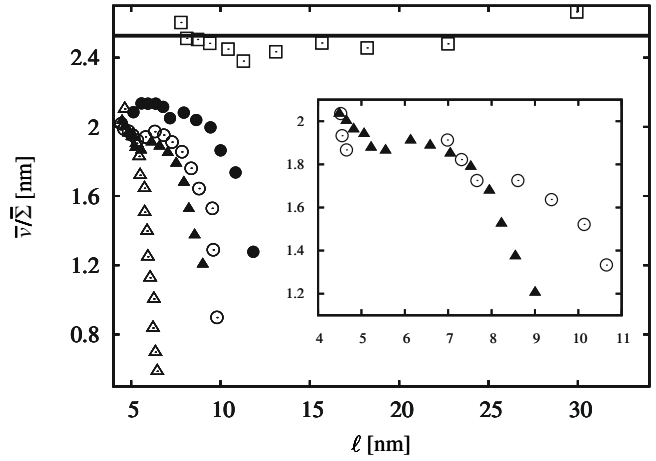

Fig. 5. Dilution law in terms of the effective volume to effective area ratio $\bar{v}/\bar{\Sigma}$ computed from $\ell\phi_{\rm lip}/2$ for the system with Simulsol $n = 6$ and various bilayer compositions: L89/S11 (△), L56/S44 (▲), L37/S63 (○), L27/S73 (●) and L0/S100 (□). The horizontal line corresponds to half the geometric thickness of the pure Simulsol $n = 6$ bilayer $\delta/2 \approx 2.53$ nm. Inset: Comparison between Simulsol $n = 6$ (▲) and $n = 16$ (○) for bilayer compositions L56/S44 and L80/S20, respectively.

interface. Because of the structure periodicity, the bilayer volume fraction $\phi_{\rm lip}$ is locally expressed as

$$\phi_{\rm lip} = \frac{N_L v_L + N_S v_S}{\mathcal{A}\ell}\,, \tag{4}$$

with, similarly

$$2\mathcal{A} = N_L \Sigma_L + N_S \Sigma_S. \tag{5}$$

This results in a geometric dilution law of the following form:

$$\ell = 2\frac{\bar{v}}{\bar{\Sigma}} \times \frac{1}{\phi_{\rm lip}}\,, \tag{6}$$

where $\bar{v}$ is an effective molecular volume $xv_S + (1-x)v_L$, $\bar{\Sigma}$ an effective interfacial molecular area $x\Sigma_S + (1-x)\Sigma_L$ and x denotes the mole fraction of species S in the mixed bilayer. From eq. (6) rephrased as $\bar{v}/\bar{\Sigma} = \ell\phi_{\rm lip}/2$, the non-linear dilution laws displayed in figs. 3 and 4 for Simulsol $n = 6$ point to confinement-induced changes in the *lateral* stacking properties of the molecules within a bilayer, *i.e.* changes in Σ_S or Σ_L values, as incompressibility ensures that v_L and v_S remain constant.

According to the geometric considerations leading to eq. (6) above, it appears significant to display the dilution law in terms of $\ell\phi_{\rm lip}/2$ as a function of hydration, as in fig. 5. Such a representation indeed evidences for the system under study the coupling between vertical, hydration-driven, and lateral confinement of the molecules self-assembled in stacked bilayers. Except for pure Simulsol $n = 6$ where a (nearly constant) bilayer thickness can be defined by the ratio $2v_S/\Sigma_S$, which implies a constant interfacial area per Simulsol molecule Σ_S and, therefore, bilayers loosely coupled across solvent layers whatever the hydration level, the bilayers are *strongly* coupled along z for all other bilayer compositions. Such a strong coupling is, of course, quite common in the lamellar stacks of *pure* lipids [37, 38], which usually cannot incorporate large amounts of solvent, and it is indeed observed here with pure lecithin (L100/S0 system, $v_L/\Sigma_L \equiv \ell\phi_{\rm lip}/2$ in the order of 1.9 nm—data not shown). It is also interesting to notice that, for the bilayer composition L56/S44 and Simulsol $n = 6$, $\ell\phi_{\rm lip}/2$ is nearly constant (with a value ≈ 1.8 nm) in the hydration range where a lamellar-lamellar phase coexistence is observed with a similar bilayer composition and Simulsol $n = 16$. We come back to these points when discussing bilayer fluctuations and electronic structure, sects. 3.3 and 3.4 below.

Replacing Simulsol $\langle n\rangle = 10$ by a co-surfactant with a shorter hydrophilic head $n = 6$ yields to a clear effect on the dilution limit of the system: The limiting stacking period $\ell_{\rm max}$ beyond which any amount of additional solvent cannot be incorporated within the lamellar structure and remains in excess *monotonically* increases with the amount of Simulsol $n = 6$ in the bilayers. It is even possible that $\ell_{\rm max}$ for the pure Simulsol system L0/S100 is infinite—in any case too large to be measured with our present experimental capabilities. Such a behaviour is to be expected when approaching or crossing the so-called unbinding transition [39–41] where long-range thermally induced undulation (repulsive) interactions between bilayers overcome attractive (*e.g.* van der Waals) interactions. In sect. 3.3 below, we characterise bilayer flexibility and interactions by means of the Caillé parameter, and discuss the unbinding transition in more quantitative details.

3.3 Fluctuating stacked bilayers

For the reasons given in the Introduction, the elastic properties of a lamellar stack of bilayers are key to understanding the stability of such self-assembled systems. They also control the magnitude of thermally induced fluctuations in bilayer conformation ("undulation" fluctuations) and inter-bilayer separation ("compression/dilation" fluctuations). The Caillé parameter η is useful for characterising those fluctuations, albeit not completely because undulation and compression/dilation elastic constants are merged together in its expression, eq. (1).

From the data displayed in fig. 6 for Simulsol $n = 6$ and bilayer composition L56/S44, a conspicuous change in the regime of bilayer fluctuations can be spotted at a stacking parameter ℓ^* about 6 nm, corresponding to $\phi_{\rm lip} = 0.6$. Less hydrated samples are indeed characterised by the "confined" type diffractograms of sect. 3.1, "swollen" type diffractograms being associated to more hydrated systems. With again the exception of the *pure* L0/S100 Simulsol $n = 6$ system—where "swollen" type diffractograms are observed along the whole dilution line—, a similar kink in the $\eta(\ell)$ curves is observed for all other bilayer compositions, with ℓ^* increasing from ≈ 5.6 nm to ≈ 6.8 nm when the lecithin content decreases from 89% to 27%.

Despite the above-mentioned singular case of the L0/S100 system, the overall evolution of the Caillé

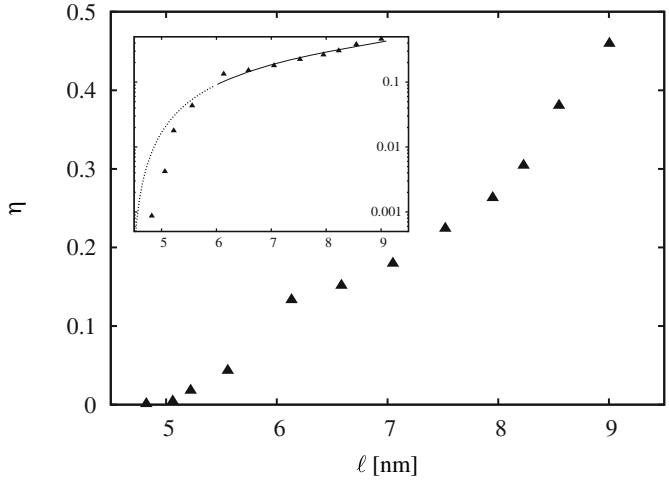

Fig. 6. Caillé parameter as a function of hydration for the Simulsol $n = 6$ system with bilayer composition L56/S44. Inset: The continuous line is a fit to the Milner-Roux model—see text for details. Below the stacking parameter $\ell^* = 6\,\mathrm{nm}$ where diffractograms are typical of "collapsed" bilayers, the extrapolated model is displayed as a dotted line.

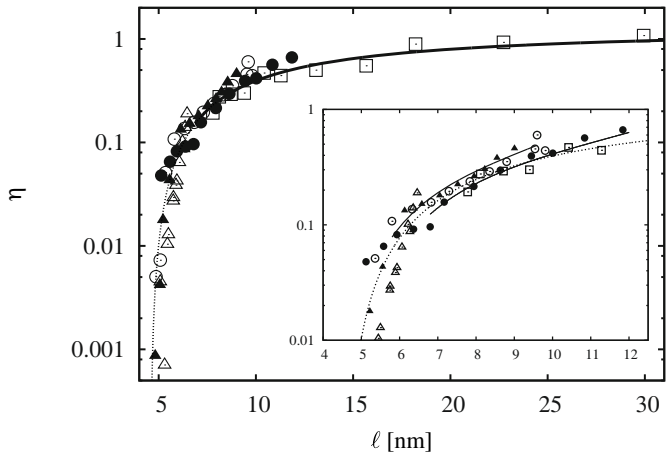

Fig. 7. Caillé parameter as a function of hydration for the Simulsol $n = 6$ system and bilayer compositions L89/S11 (△), L56/S44 (▲), L37/S63 (○), L27/S73 (●), L0/S100 (□). The thick line is a fit of eq. (8) to data corresponding to the pure Simulsol system (□). The dotted line is an extrapolation of the same equation to smaller values of ℓ where pure Simulsol bilayers do not stack yet in a lamellar structure. Inset: Close-up of the same data for lesser hydration. The dotted line is drawn according to eq. (8), while the two thick lines are fits of the Milner-Roux model, eq. (13), to the L37/S63 (○) and L27/S73 (●) data ("swollen" type diffractograms only), with $\delta = 4.4\,\mathrm{nm}$, $\ell_{\max} = 9.6\,\mathrm{nm}$ and $\delta = 4.7\,\mathrm{nm}$, $\ell_{\max} = 12\,\mathrm{nm}$, respectively.

parameter with hydration and bilayer composition somehow follows a kind of "universal" behaviour, shown in fig. 7, as already observed with the longer Simulsol $\langle n \rangle = 10$ [26].

It is worth mentioning here that a truly universal behaviour for the Caillé parameter is the natural consequence of eq. (2) and eq. (3) when the *only* relevant interaction between bilayers stems from Helfrich undulation mechanism, that is to say the configurational entropy loss resulting from "collisions" between adjacent bilayers, somehow similarly to the mechanism leading to a universal pressure law for ideal gases. In this particular case, the free energy per unit bilayer area associated to sterically restricted bilayer undulations in a lamellar stack of period ℓ expresses as [7–9]

$$V_H(\ell) = \frac{3\pi^2}{128}\frac{(k_BT)^2}{\kappa}\frac{1}{(\ell - \delta_\mathrm{u})^2}\,. \tag{7}$$

In eq. (7) δ_u, mathematically defined as a limiting minimum value for ℓ, is physically to be interpreted as the *steric* thickness of the bilayers: When ℓ reaches δ_u, undulation fluctuations are sterically wholly forbidden and the free energy becomes infinite[3].

With the definition for η given by eq. (1), eq. (7) immediately leads to

$$\eta = \frac{4}{3}\left(1 - \frac{\delta_\mathrm{u}}{\ell}\right)^2, \tag{8}$$

an expression "universal" in the sense that it does not dependent on the bilayer bending modulus κ, a system-dependent property. The continuous line drawn in fig. 7 corresponds to the model of eq. (8), with parameter δ_u fitted to the data for the pure L0/S100 Simulsol system. The fitted value is found to be 4.6 nm, reasonably close to the value $\delta \approx 5.1\,\mathrm{nm}$ resulting from the analysis of the dilution law for the same system, sect. 3.2. Somehow unexpectedly, the model also apparently gives a broadly satisfactory description for *all* η values, that is to say even when direct couplings between adjacent bilayers—presumably by means of long-range van der Waals attractions or polymer-mediated steric repulsions—cannot be neglected as shown in the discussion following fig. 5, sect. 3.2.

Taking into account in a *perturbative* way van der Waals attractions between lipid bilayers (and, possibly, other relevant interactions), as proposed by Milner and Roux in ref. [41], provides an argument for—at least, partially—interpreting the latter observation. In this approach, a virial-like term, expressed to the lowest perturbative order as $-k_BT\chi\phi_\mathrm{lip}^2$, is merely added to the Helfrich free energy per unit volume of the lamellar stack. Parameter χ here is analogous to the correction to the hard-sphere result for the virial coefficient in the thermodynamic description of non-ideal gases, and is defined to be *positive* in the presence of *attractive* interactions [41]. In terms of free energy per unit bilayer *area*, eq. (7) is thus to be replaced by:

$$V(\ell, \phi_\mathrm{lip}) = V_H(\ell) - \ell \times k_BT\chi\phi_\mathrm{lip}^2 \tag{9}$$

since there is exactly one piece of bilayer with area $\mathcal{A}$ in the cylindrical volume of height ℓ extending along the stacking axis above a base $\mathcal{A}$.

It is important to pay due attention to the immediate and unavoidable consequence of such a "virial" approach:

[3] In the gas analogy, the excluded-volume parameter of the van der Waals pressure equation plays a role very similar to δ_u.

The free energy now intrinsically depends on *two* independent variables, namely ℓ and $\phi_{\rm lip}$, with the dilution law, namely the relation between ℓ and $\phi_{\rm lip}$, in principle to be deduced from the overall thermodynamic properties of the system. In the present case, as discussed in sect. 3.2, longitudinal and lateral confinements (as quantified by ℓ and, for instance, the effective volume to effective area ratio $\bar{v}/\bar{\Sigma}$, respectively) are strongly coupled and this implies explicitly taking into account the thermodynamic contribution of the in-plane stretching of bilayers to the system free energy [42]. On the other hand, the validity of the virial expansion requires interactions between bilayers to be, somehow, "weak" enough to be treated perturbatively. In such a limit, the dilution law is expected to be of the simple form $\ell \propto 1/\phi_{\rm lip}$.

Fostered by the considerable success—at least, qualitatively speaking—of the van der Waals model of non-ideal gases in describing the liquid-gas phase separation, a phenomenon well beyond the *a priori* validity of the perturbative hypotheses, we tentatively use the virial approach to the thermodynamics of lamellar stacks by altogether neglecting the effects of interactions on the dilution law. In other words, we *assume* in the following that ℓ and $\phi_{\rm lip}$ are actually not independent variables and, therefore, still use eq. (3) in order to compute the compression modulus B.

Ignoring for simplicity the difference between "geometric" $\delta \equiv \ell\phi_{\rm lip}$ and "steric" $\delta_{\rm u}$ bilayer thicknesses, the compression modulus is readily obtained as

$$B = \frac{9\pi^2}{64}\frac{(k_BT)^2}{\kappa}\frac{\ell}{(\ell-\delta)^4} - 2k_BT\chi\frac{\delta^2}{\ell^2}\,. \qquad (10)$$

In strong analogy with non-ideal gases in the presence of attractive interactions, the virial approach to undulating lamellar stacks of bilayers implies, when χ is positive, the existence of a *dilution limit*, that is to say a maximal $\ell_{\rm max}$ (or a maximal amount of solvent) beyond which any added solvent will phase-separate with a lamellar stack of period $\ell_{\rm max}$ [41]. A common tangent construct with the free energy per unit volume drawn as a function of $\phi_{\rm lip}$ leads to the following relation:

$$\frac{3\pi^2}{64}\frac{k_BT}{\kappa}\frac{\phi^*_{\rm lip}}{(1-\phi^*_{\rm lip})^3} = \chi\delta^3 \qquad (11)$$

between the lipid volume fraction at the dilution limit, $\phi^*_{\rm lip}$, and the other physical parameters characterising the lamellar stack. In terms of stacking period, $\ell = \delta/\phi_{\rm lip}$ and, therefore, $\ell_{\rm max} = \delta/\phi^*_{\rm lip}$, eq. (11) may then be used to eliminate the (positive) parameter χ in eq. (10). The compression modulus expression is thus recast as

$$B = \frac{9\pi^2}{64}\frac{(k_BT)^2}{\kappa}\frac{\ell}{(\ell-\delta)^4} \times\left\{1-\frac{2}{3}\left(\frac{\ell_{\rm max}}{\ell}\right)^2\frac{(\ell-\delta)^4}{\ell(\ell_{\rm max}-\delta)^3}\right\}. \qquad (12)$$

Note that the unpertubed limit where $\chi = 0$—eq. (9) merges with eq. (7)—corresponds to $\phi^*_{\rm lip} = 0$ as a solution to eq. (11) and, therefore, $\ell_{\rm max}$ being formally *infinite*.

Table 1. Parameters δ and $\ell_{\rm max}$ from the Helfrich limit (L0/S100 sample, where $\ell_{\rm max}$ is actually *infinite*—see remark below eq. (12)) or full Milner-Roux description of the Caillé exponent η—other samples, except L89/S11 that cannot be described by eq. (13). For sample L89/S11, the value $\ell_{\rm max}$ then comes from the dilution law data. Parameter $2\bar{v}/\bar{\Sigma}$ is a rough estimate for the geometric bilayer thickness coming from data displayed in fig. 5. Stacking parameter ℓ^* separates "confined" from "swollen" type diffractograms. All values in nanometres.

	$2\bar{v}/\bar{\Sigma}$	δ	ℓ^*	$\ell_{\rm max}$
L89/S11	≈ 2.6	**undef.**	5.6	**6.5**
L56/S44	≈ 3.0	4.4	6.0	9.1
L37/S63	≈ 3.1	4.4	5.8	9.6
L27/S73	≈ 3.2	4.7	6.8	12.0
L0/S100	≈ 5.1	4.6	< 7.8	$+\infty$

Because the present approach almost entirely neglects the coupling between adjacent bilayers, apart from the perturbative virial contribution, it seems adequate to keep eq. (2) as a valid description of the smectic splay constant K. With this last hypothesis, the Caillé exponent is predicted to be

$$\eta = \frac{4}{3}\left(1-\frac{\delta}{\ell}\right)^2 \times\left\{1-\frac{2}{3}\left(\frac{\ell_{\rm max}}{\ell}\right)^2\frac{(\ell-\delta)^4}{\ell(\ell_{\rm max}-\delta)^3}\right\}^{-1/2}. \qquad (13)$$

Even though, similarly to the shortcomings of the van der Waals theory of non-ideal gases, a wholly *quantitative* and rigorous description of the lamellar phase is missing, fig. 6 as well as the inset in fig. 7 quite convincingly illustrate the capabilities of the perturbative Milner-Roux approach for predicting, at least when ℓ remains greater than ℓ^*, the evolution with hydration of the Caillé exponent when not too strong attractive interactions effectively bind the stacked bilayers at a finite dilution limit $\ell_{\rm max}$. Fitted values of the parameter δ clearly often overestimate their closest experimental counterpart, namely $2\bar{v}/\bar{\Sigma}$ (fig. 5), but dilution limit parameters $\ell_{\rm max}$ are nicely consistent with the experimental estimates that can be read in fig. 4 or 5—see table 1 for the relevant numerical values. In addition, the departure *from above* from the simple prediction of eq. (8) is very satisfactorily described in the high-hydration side of the dilution range.

3.4 Bilayer electronic structure

Apart from the structure factor parameters ℓ and η discussed in the previous two Sections, *form factor* parameters are also derived form the diffractogram analysis. In the double-square well model of the electronic structure used here [27,43], these amount to two heights δ_H, δ_T, and one contrast ratio r_ρ—see also sect. 3.1 and fig. 2. It will turn out convenient to consider the "scattering" thickness

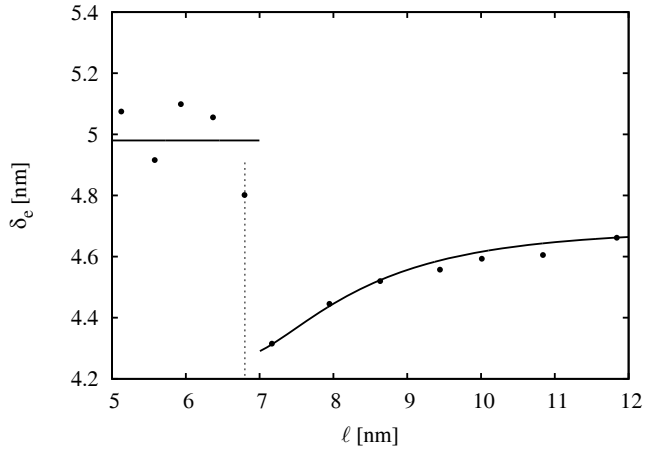

Fig. 8. Scattering thickness δ_e as a function of hydration for the Simulsol $n = 6$ system with bilayer composition L27/S73. The ℓ^* value separating "collapsed" from "swollen" type diffractograms is marked by the vertical dotted line. The continuous lines are guides for the eye.

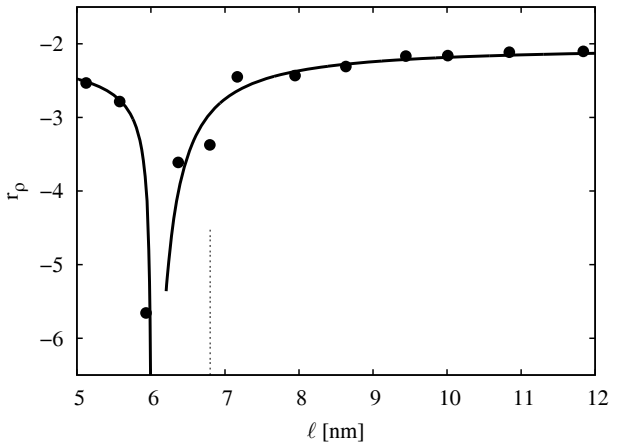

Fig. 9. Variation with hydration of the bilayer contrast ratio r_ρ for the Simulsol $n = 6$ system with bilayer composition L27/S73. The ℓ^* value separating "collapsed" from "swollen" type diffractograms is marked by the vertical dotted line. The continuous lines are guides for the eye.

δ_e of a bilayer, defined by $\delta_e = 2(\delta_H + \delta_T)$, presumably close, but not necessarily equal, to the other two bilayer geometric characteristics introduced previously, namely the "dilution law" thickness or $\ell\phi_{lip}$ (sect. 3.2) and the "steric" thickness δ_u (sect. 3.3).

Figures 8 and 9 illustrate for the Simulsol $n = 6$ system with bilayer composition L27/L73 the evolution of the scattering thickness δ_e and contrast ratio r_ρ parameters, respectively, when hydration increases. As expected for the typical "core-shell" electronic density contrast of amphiphilic bilayers self-assembled in water, the parameter r_ρ remains *negative* along the whole dilution line. The *non-monotonous* behaviour here observed for both δ_e and r_ρ, however, is quite conspicuous. In particular, it is not readily apparent for the bilayer thickness associated to the dilution law, $\ell\phi_{lip}$ (or $2\bar{v}/\bar{\Sigma}$), compare with fig. 5 in sect. 3.2. Still, characteristic values for the stacking period, separating two distinct regimes, may be defined: At low hydration the form factor parameters δ_e and r_ρ are constant—or decreasing—when hydration increases, whereas both increase significantly at higher hydration. The precise *value* for the stacking period between the two regimes is not found to be the same in the two data sets, but falls in the range 6–7 nm, typically associated to a lipid volume fraction around 0.65. It is also quite close to parameter ℓ^* that separates "confined" bilayer systems from "swollen" ones—see sects. 3.1 and 3.3—and will therefore be represented by the same symbol.

From these converging experimental evidences, we propose that a *vertical* confinement-induced transition in the surfactant chain conformation is at the origin of the distinction between "confined" and "swollen" bilayer stacks. As already suggested in ref. [26], the polar (non-ionic) part of Simulsol may be considered as a (short) polymer grafted onto any of the two bilayer-solvent interfaces of each bilayer, with "mushroom" or "brush" conformations depending on the grafting density, *i.e.* composition-driven *lateral* confinement. For such a simple view to be correct, however, adjacent bilayers should *not* be coupled by, say, overlapping chains belonging to distinct bilayers. Qualitatively speaking, *three* regimes for the hydrophilic component of the bilayers have thus to be distinguished as a function of hydration:

High hydration limit: The amount of water between bilayers is large enough for the grafted polymer to be in its unperturbed conformation—either "mushroom"-like or "brush"-like, depending on grafting density. Bilayers interact only weakly. The "virial" approach should be valid. In this regime, both δ_e and r_ρ are expected to remain constant.

Medium hydration range: "Mushrooms" (or "brushes", depending on bilayer composition) from adjacent bilayers start to overlap in their common water channel. Because water at room temperature is a good solvent for ethoxylated chains, there is an effective repulsion between chains, with consequently a lesser vertical extension for either the "mushrooms" or the "brushes" if enough space is left for them to spread laterally. The bilayer hydrophilic thickness (as described by parameter δ_H) decreases when hydration decreases. As the polar part of Simulsol now crowds the *whole* water channel, the double-square well model for the electronic density presumably becomes less adequate but, if still used, it also predicts that the contrast parameter $\Delta\varrho_H$ *decreases* when hydration decreases. This somehow counter-intuitive property results from the "solvent" layer in the contrast model being *richer* in electrons, as compared to pure water, because it now hosts a fraction of the ethoxylated chains grafted onto the bilayers. The stronger interactions between closer bilayers do not affect yet parameter δ_T (describing the bilayer hydro*phobic* component) and, because the reference level in the solvent layer has changed, the contrast parameter $\Delta\varrho_T$ becomes even more negative. In this

regime, both δ_e and r_ρ gradually decrease when hydration decrease. Though *stricto sensu* no longer valid, the "virial" approach to bilayer interactions keeps its heuristic usefulness.

Highly dehydrated limit: Ethoxylated chains from adjacent bilayers overlap strongly and the distinction between "mushroom" and "brush" conformations is no longer relevant. In the now highly crowded water-containing channels, the polar heads of *lecithin* also interact strongly. This leads to a rather drastic change in lipid and surfactant molecular conformations that our present approach cannot fully apprehend. Tentatively still using the (rather primitive in this context) double-square well, bilayer—solvent model, such a drastic change is indirectly evidenced by the cusp (in $\eta(\ell)$ data) or jump (as far as δ_e or r_ρ are concerned) associated to what appears as a transition from "swollen" to "confined" lamellar stacks.

All the available data is broadly consistent with the above-described scheme. In particular, implicit for the high hydration regime, and assumed at medium hydration, parameter δ_T associated to bilayer hydrophobic components indeed remains nearly constant (within $\pm 5\%$, data not shown) in the corresponding hydration ranges. In addition, the dilution features of parameters δ_e or r_ρ follow similar trends as displayed in figs. 8 and 9, respectively, whatever the bilayer lecithin-to-Simulsol composition ratio—except that dilution lines may be truncated at high (with lecithin-rich samples) or low (pure Simulsol system) hydration.

A tendency for ℓ^* to increase with the amount of Simulsol incorporated into the bilayers, already observed when first discussing the "confined"-to-"swollen" transition in terms of Caillé exponent, may also be detected in those $\delta_e(\ell)$ and $r_\rho(\ell)$ curves where ℓ^* is clearly marked. A (tentative) explanation for this behaviour may be sought in the theoretical description of compressed brushes given in ref. [44]. In the limit where $h/h^* \ll 1$, where h is half the separation between two parallel plates, each bearing grafted polymer layers with an equilibrium thickness h^*, the free energy per grafted chain is given, in reduced units, by [44]

$$\mathcal{F} = N^2 w\sigma/h, \tag{14}$$

where N is the number of monomers per chain, w the excluded-volume parameter and σ the surface coverage. If the brush analogy is relevant for Simulsol hydrophilic heads interacting across the water channels of a (highly dehydrated) lamellar stack, then surface coverage σ increases with the bilayer Simulsol content x, and h should be identified with $\ell/2 - \delta_T$. The drastic change in bilayer structure taking place when ℓ becomes smaller than ℓ^* could be induced by the free energy per chain, eq. (14), reaching a critical threshold $\mathcal{F}^*$. This hypothesis would lead to the prediction

$$\ell^* = 2\left(\delta_T + \frac{N^2 w\sigma}{\mathcal{F}^*}\right), \tag{15}$$

in qualitative agreement with observations since δ_T does not vary strongly with bilayer composition.

4 Conclusion

The interplay between soft confinement and steric effects has been studied in lamellar stacks of mixed lecithin-Simulsol bilayers, varying both hydration and bilayer composition, that is to say both *vertical* and *lateral* confinement of the co-surfactant.

Apart from its well-documented role in increasing bilayer flexibility, the co-surfactant also has a clear effect on bilayer *interactions*, increasing their repulsive component. This effect is directly observed from the increase of the dilution limit $\ell_{\max}$ with Simulsol content, as well as indirectly, from the Caillé exponent values η extracted by modelling the X-ray diffractograms [27, 28].

Interactions between bilayers are satisfactorily described, at least at higher hydration, in the virial approach of the so-called "unbinding" transition proposed by Milner and Roux [41].

In the highly dehydrated limit where, for steric reasons, the vertical confinement of the hydrophilic components of the bilayer is strongly coupled to the lateral confinement, a structural transition occurring in the lipid and co-surfactant molecular conformations is invoked as a mechanism to explain the evolution, observed experimentally, from "swollen" to "confined" regimes. The bilayer structural transition may be triggered by the "brush" compression energy stored in the Simulsol hydrophilic block, a hypothesis that remains to be confirmed by systematically varying the hydrophilic block length n—an experimental study presently in progress.

The bilayer structural transition may also explain the lamellar-lamellar phase coexistence observed at low hydration with longer Simulsol molecules. Indeed, as has been shown by Silva *et al.* [45] in the context of *catanionic* lamellar structures in water, confinement effects with a strong impact on bilayer structure—through a counter-ion condensation mechanism in ref. [45]—and, consequently, on interactions between bilayers may lead to such phase coexistences. The influence of the Simulsol hydrophilic block length n, as well as Simulsol content in the mixed bilayers on the phase separation phenomenon is therefore of definite interest. The corresponding study has been undertaken.

Overall, a better knowledge of the lamellar stack free energy would be desirable, in particular for a better description of the dilution law when vertical and lateral confinement effects are strongly coupled, which is the common situation for most of the studied systems. Such a knowledge may help in understanding the occurrence of "confined" and "swollen" systems and, specifically, the lamellar-lamellar phase coexistence at low hydration observed with longer Simulsol, which may be associated to the ability of the mixed lipid-Simulsol layered structure to bind, *e.g.* DNA fragments [23–25].

Author contribution statement

All authors contributed equally to the present work.

The support by Fundação de Amparo à Pesquisa do Estado de São Paulo through grant 2011/16149-8 is gratefully acknowledged. We also thank IdEx Bordeaux (France) and Conselho Nacional de Desenvolvimento Científico e Tecnológico (Brazil) for providing support through their respective programs "Doctorat international" and "Ciência sem Fronteiras", as well as company SEPPIC for kindly providing us the size-sorted Simulsols used in this study.

References

1. R. Jelinek, S. Kolusheva, Biotechnol. Adv. **19**, 109 (2001).
2. E. Sackmann, Science **271**, 43 (1996).
3. G. Scolan, PhD in pharmacy: *Applications nanobiotechnologie et thérapeutiques des membranes en bicouches lipidiques* (Grenoble, 2012).
4. D.P. Nikolelis, T. Hianik, U.J. Krull, Electroanalysis **11**, 7 (1999).
5. M. Mezei, V. Gulasekharam, Life Sci. **26**, 1473 (1980).
6. S. Akhtar, R.L. Juliano, J. Controll. Release **22**, 47 (1992).
7. W. Helfrich, Z. Naturforsch **33a**, 305 (1978).
8. C.R. Safinya, D. Roux, G.S. Smith, S.K. Sinha, P. Dimon, N.A. Clark, A.-M. Bellocq, Phys. Rev. Lett. **57**, 2718 (1986).
9. D. Roux, C.R. Safinya, J. Phys. (Paris) **49**, 307 (1988).
10. I. Szleifer, D. Kramer, A. Ben-Shaul, D. Roux, W.M. Gelbart, Phys. Rev. Lett. **60**, 1966 (1988).
11. M.B. Schneider, J.T. Jenkins, W.W. Webb, J. Phys. (Paris) **45**, 1457 (1984).
12. C.R. Safinya, E.B. Sirota, D. Roux, G.S. Smith, Phys. Rev. Lett. **62**, 1134 (1989).
13. M. Winterhalter, W. Helfrich, J. Phys. Chem. **92**, 6865 (1988).
14. J.L. Harden, C. Marques, J.-F. Joanny, Langmuir **8**, 1170 (1992).
15. H.N.W. Lekkerkerker, Physica A **140**, 319 (1989).
16. S.T. Milner, T.A. Witten, J. Phys. (Paris) **49**, 1951 (1988).
17. J.T. Brooks, M.E. Cates, J. Chem. Phys. **99**, 5467 (1993).
18. F. Clement, J.-F. Joanny, J. Phys. II **7**, 973 (1997).
19. P. Kekicheff, B. Cabane, M. Rawiso, J. Colloid Interface Sci. **102**, 51 (1984).
20. E.Z. Radlinska, T. Gulik-Krzywicki, F. Lafuma, D. Langevin, W. Urbach, C.E. William, R. Ober, Phys. Rev. Lett. **74**, 4237 (1995).
21. M.-F. Ficheux, A.-M. Bellocq, F. Nallet, J. Phys. II **5**, 823 (1995).
22. C. Ligoure, G. Bouglet, G. Porte, O. Diat, J. Phys. II **7**, 473 (1997).
23. T. Pott, A. Colin, L. Navailles, D. Roux, Interface Sci. **11**, 249 (2003).
24. E. Andreoli de Oliveira, E.R. Teixeira da Silva, A. Février, E. Grelet, F. Nallet, L. Navailles, EPL **91**, 28001 (2010).
25. E.R. Teixeira da Silva, E. Andreoli de Oliveira, A. Février, F. Nallet, L. Navailles, Eur. Phys. J. E **34**, 83 (2011).
26. B.B. Gerbelli, R.L. Rubim, E.R. Silva, F. Nallet, L. Navailles, C.L.P. Oliveira, E.A. de Oliveira, Langmuir **29**, 13717 (2013).
27. F. Nallet, R. Laversanne, D. Roux, J. Phys. II **3**, 487 (1993).
28. C.L.P. Oliveira, B.B. Gerbelli, E.R.T. Silva, F. Nallet, L. Navailles, E.A. Oliveira, J.-S. Pedersen, J. Appl. Crystallogr. **45**, 1278 (2012).
29. A. Caillé, C. R. Hebdo. Acad. Sci. Paris B **274**, 891 (1972).
30. F. Nallet, D. Roux, J. Prost, J. Phys. (Paris) **50**, 3147 (1989).
31. F. Nallet, D. Roux, C. Quilliet, P. Fabre, S.T. Milner, J. Phys. II **4**, 1477 (1994).
32. C. Ligoure, J. Phys.: Condens. Matter **17**, S2911 (2005).
33. W. Helfrich, R.M. Servuss, Nuovo Cimento **3**, 137 (1984).
34. R. Strey, R. Schomäcker, D. Roux, F. Nallet, U. Olsson, J. Chem. Soc. Faraday Trans. **86**, 2253 (1990).
35. D. Roux, F. Nallet, É. Freyssingeas, G. Porte, P. Bassereau, M. Skouri, J. Marignan, Europhys. Lett. **17**, 575 (1992).
36. É. Freyssingeas, D. Roux, F. Nallet, J. Phys.: Condens. Matter **8**, 2801 (1996).
37. V. Luzzati, H. Mustacchi, A. Skoulios, F. Husson, Acta Cryst. **13**, 660 (1960).
38. V. Luzzati, F. Husson, J. Cell Biol. **19**, 207 (1962).
39. R. Lipowsky, S. Leibler, Phys. Rev. Lett. **56**, 2541 (1986).
40. R. Podgornik, V.A. Parsegian, Langmuir **8**, 557 (1992).
41. S.T. Milner, D. Roux, J. Phys. I **2**, 1741 (1992).
42. V.A. Parsegian, N. Fuller, R.P. Rand, Proc. Natl. Acad. Sci. U.S.A. **76**, 2750 (1979).
43. T. Gulik-Krzywicki, E. Rivas, V. Luzzati, J. Mol. Biol. **27**, 303 (1967).
44. S.T. Milner, T.A. Witten, M.E. Cates, Macromolecules **21**, 2610 (1988).
45. B.F.B. Silva, E.F. Marques, U. Olsson, J. Phys. Chem. B **111**, 13520 (2007).